Regression analysis of the vibroarthrogram in the external load conditions

Adam Łysiak[1]*, Dawid Bączkowicz[2], Dorota Borzucka[2],
Mirosław Szmajda[1], Aleksandra Kawala-Sterniuk[3],
Sebastian Brol[4], Michał Dołęgowski[1], Janusz Mroczka[1]

[1] Faculty of Electrical Engineering, Automatic Control and Computer Science, Opole University of Technology, Prószkowska 76, 45-758 Opole, Poland
[2] Faculty of Physical Education and Physiotherapy, Opole University of Technology, Prószkowska 76, 45-758 Opole, Poland
[3] Department of Artificial Intelligence, Faculty of Information and Communication Technology, Wroclaw University of Science and Technology, Wybrzeże Wyspiańskiego 27, 50-370 Wrocław, Poland
[4] Faculty of Mechanical Engineering, Opole University of Technology, Mikołajczyka 5, 45-271 Opole, Poland
* Corresponding author's e-mail: a.lysiak@po.edu.pl

ABSTRACT

Due to the critical function and susceptibility to loading-related issues of the knee joint, the development of novel examination methods is beneficial. Vibroarthrography (VAG) is a method for analyzing vibrations generated by the knee joint in motion. While extensive literature exists on VAG analysis in the discrete, classification context, this study analyzed VAG signals in a regression, i.e., continuous one. Such approach allows for more nuanced analysis, providing qualitative conclusions. The relationship was investigated between VAG signals and external loads in asymptomatic male participants performing squats with varying weights. A sample of 38 male asymptomatic participants was analyzed, with each participant executing 8 sets of squat exercises with different loads (from 0 to 70 kg with 10 kg increments; random ordering across participants). Linear mixed models regression analysis was used to model the relationships between selected VAG features and external loads, providing quantitative insights into the mechanical function of the knee joint. The analysis showed that power of the signal is positively correlated with external load, and lower frequencies contain proportionally more power with increasing load. These findings suggest that VAG may serve as a sensitive tool for detecting changes in joint arthrokinematics under varying loads. The regression analysis provided quantitative insights and continuous relationships, offering potential for clinical decision support systems in evaluating joint function and personalized treatment planning.

Keywords: vibroarthrography, mixed models, external load, knee joint, frequency range maps, power features.

INTRODUCTION

Vibroarthrography

The knee joint is one of the most heavily loaded joints in the human body [1, 2]. It is, therefore, highly susceptible to various kinds of injuries [3, 1]. And, since hyaline cartilage is in most part devoid of nerves [4], micro-injuries generally do not cause pain and remain unnoticed [5, 6]. During movement, however, they do generate micro-vibrations that can be registered by an accelerometer attached to the knee-joint. Analysis of those vibrations is called vibroarthrography (VAG), and vibroarthrogram is referring to the registered vibration signal. Unlike standard diagnostic methods, such as the X-ray or magnetic resonance imaging, vibroarthrography examines articular connections in a dynamic way, i.e. during movement, providing information about the function of the joint rather than its structure. Nonetheless, it is generally agreed that artifacts

(like spikes or low-amplitude high-frequency oscillations) in signals correspond to, or are made by, abnormalities in joint's structure [7–9].

Background

There is a vast literature about VAG analysis in the context of classification, mostly devoted to binary class differentiation - between symptomatic and asymptomatic groups [10]. For example, Befrui et al. [11] utilized frequency analysis with support vector machines to classify signals into asymptomatic and osteoarthritis classes, achieving 0.8 specificity and 0.75 sensitivity. More recently, Karpiński et al. [8, 9] analyzed signals from patients referred for surgical treatment due to intraarticular lesions to differentiate them from a control group. In another recent work, Machrowska et al. [12] analyzed VAG signals for detecting osteoarthritis, using ensemble empirical mode decomposition and detrended fluctuation analysis to de-noise the signals. They extracted and selected informative features using ANOVA and performed neural network classification, achieving specificity and sensitivity of up to 0.93 for both classes.

Beyond binary classification, there are multiple studies analyzing VAG signals in multi-class classification problems. For instance, Kręcisz et al. [13] created a VAG analysis system capable of differentiating five condition classes: three stages of chondromalacia patellae, osteoarthritis, and a healthy group. VAG signals can also be used to describe joint changes within the same joints. Falkowski et al. [14] successfully used vibroarthrography to evaluate the effects of intra-articular injection of hyaluronic acid.

Recent work by Ołowiana et al. [15] is particularly relevant to the current research. They studied VAG signals in asymptomatic participants during squat exercises with varying external loads (0, 10, and 20 kg), calculating four VAG features: variance mean square (VMS), Amplitude, P1, and P2 (Power Spectral Density for 50–250 Hz and 250–450 Hz frequency ranges, respectively). The study indicated that all four features are positively correlated with external load. Here, the aim is to extend this methodology by establishing specific regression lines rather than general trends.

Another relevant study is by Gharehbaghi et al. [16], who analyzed VAG signals in two groups of patients: those with Juvenile Idiopathic Arthritis (JIA) and a control group of healthy individuals. Signals were recorded during unloaded (free extension) and loaded (body weight squat) movements and evaluated using a custom knee health score based on signal features. The score ranged from 0 (healthy knee) to 1 (arthritis). They found that higher scores were observed during loaded movements for all groups, but the difference was not significant in healthy knees.

Andersen et al. [17] used linear mixed models to investigate how the positioning of sensors around the knee joint affected VAG signals. Asymptomatic participants performed flexion and extension movements with varying external loads (0–5 kg). The authors used six VAG features: average rectified value (ARV), variance of the mean square (VoMS), form factor (FF), mean power frequency (MPF), recurrence quantification analysis recurrence (REC), and determinism (DET). They found positive correlations between external load and the ARV, VoMS, FF, REC, and DET features, and a negative correlation between external load and the MPF feature. In the current research, the aim is to establish a *continuous* rather than *discrete* dependence of VAG signals on the friction between articular surfaces of the knee joint. To determine the specific nature of this dependence, VAG signals were measured during back squats with varying external loads. Figure 1 presents exemplary VAG signals measured during the squat movement without (plot *a*) and with 70 kg additional external load (plot *b*).

Research rationale and benefits

The current study builds on existing VAG research by performing regression analysis of VAG signals in relation to external loads. This approach offers a new perspective compared to previous studies, which mainly used classification methods to distinguish between different knee joint classes. By using regression, one can capture the *continuous* relationship between VAG signals and articular friction, enabling detection of subtle changes that classification methods might miss. This can enhance comprehensive biomechanical analysis. Clinically, this research could enable early intervention and personalized treatment strategies by offering a precise method to measure changes in VAG signals. Early detection of degenerative changes and micro-injuries can lead to more effective and timely interventions, improving patient outcomes. Also, continuous analysis could provide finer-grained insights into joint health, which could improve informed treatment planning and rehabilitation.
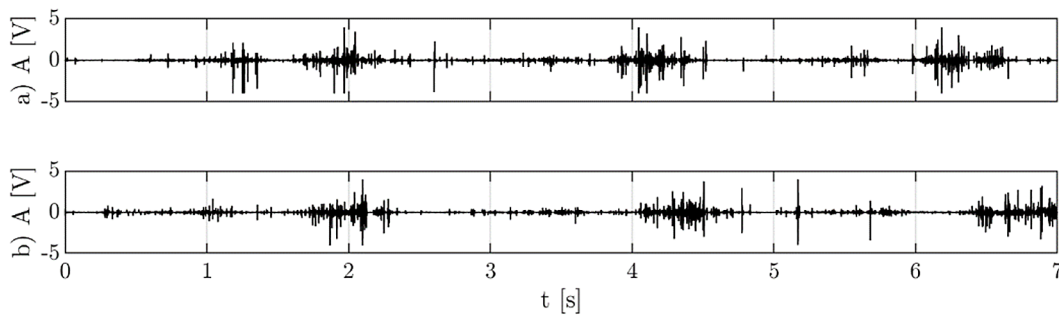
Figure 1. Exemplary VAG signals measured during the squats with: *a)* 0 kg and *b)* 70 kg external load. The loaded signal (*b*) exhibits increased variability and overall power compared to the unloaded condition (*a*), reflecting the biomechanical changes associated with higher external load. While the visual difference is subtle, these patterns align with the statistical trends in signal power and frequency distribution

Methodology

In order to test which VAG signal features were dependent on the external load, the following methodology was applied:

1. VAG signals were recorded for a sample of asymptomatic participants, during 8 trials of squat exercisewith varying external loads.
2. For every signal in the base, a feature to be tested was extracted.
3. Using obtained values of the feature, four linear models were developed:
   - simple linear model, which models just the slope of the feature's values in terms of the external load,
   - simple linear model with the free term, in which value of the intercept with the *y*-axis can be fitted to the data,
   - random intercept model, in which for every participant, the regression line can have different intercept,
   - random slope model, in which for every participant, both the intercept and the slope of the regression line can be fitted.
4. To choose the best model, Bayesian information criterion (BIC) was used [18].
5. From the best model, a goodness of fit measure was derived (R^2), as well as the parameters (intercept and slope) themselves. This allowed to measure both the variance explained by the model and rate of change of a specific feature in terms of the external load.
6. Points 1–4 were repeated for every tested feature, including time- and frequency-domain ones, as well as the Frequency Range Maps, visualizing informativeness of the whole spectrum [19].

Linear mixed effects regression models

Four linear regression models of increasing complexity were used to model changes in specific features of the vibroarthrogram in the context of increasing external load. All models were fitted to the data using Restricted Maximum Likelihood. The first, simple linear model, represents the relation between the feature and the load, assuming the intercept point at 0. This relation can be expressed by the equation:

$$X_{sl} = \beta_1 \cdot L_l + e_{sl} \qquad (1)$$

where: X_{sl} is the value of the feature for *s*-th participant, for the *l*-th load, β_1 is the slope of the model, L_l is the *l*-th load, and e_{sl} is the remaining error of the model. It is assumed, that across population, the error values are normally distributed: e_{sl} $N(0, \sigma_e^2)$, where σ_e^2 is the standard deviation of error across all participants. In the second model, a free term is added, allowing values of the intercept other than 0, giving the expression:

$$X_{sl} = \beta_0 + \beta_1 \cdot L_l + e_{sl} \qquad (2)$$

where: β_0 is the intercept value.

The third model includes additional random intercept term. This addition allows to model changes in the feature's values with the separate intercept for every participant. The model is expressed as follows:

$$X_{sl} = \beta_0 + S_{0s} + \beta_1 \cdot L_l + e_{sl} \qquad (3)$$

where: the S_{0s} is the specific intercept deviation of the *s*-th participant from the average (β_0) value. It is assumed that across

participants, values of the intercept are distributed normally, i.e.: $S_{0l} \, N(0, \sigma^2_{S\,0})$, where $\sigma^2_{S\,0}$ is the standard deviation of the intercept for the whole population.

The forth model additionally allows slope to vary across participants. It is expressed by:

$$X_{sl} = \beta_0 + S_{0s} + $$
$$+ (\beta_1 + S_{1s}) \cdot L_l + e_{sl} \qquad (4)$$

where: the S_{1s} is the deviation of the s-th participant form the average slope value, i.e. β_1. Again, distribution of the slope values across the population is assumed to be normal: $S_{1l} \, N(0, \sigma^2_{S\,1})$, where $\sigma^2_{S\,1}$ is the standard deviation of slope values across the population.

Inclusion of the random terms in models, i.e. S_{0s} and S_{1s}, allows to draw conclusions not only about the general trends across population, but also about the dispersion of those terms across population. One can say, for example, not only that the general trend of some specific feature is positively correlated with the external load (given that the β_1 coefficient is positive), but also that the correlations across the population are consistently positive or not, given low or high standard deviation of S_{1s} term, respectively. The standard deviation, therefore, provides additional information about the variability of correlations within the population.

Goodness of fit measures

To evaluate how well the models represented changes in the features' values, a conditional R^2 goodness of fit measure was acquired for each model. It can be interpreted as a variance explained by the model, using both fixed and random effects [20, 21] (precise definition will be provided later).

Inclusion of more terms in models guarantees better fit to the data. In order to avoid overfitting, the BIC [18] was used. Essentially, BIC penalizes the number of terms, promoting simpler models, and rewards lower error, promoting more accurate models [22].

Signal's features

Time-domain features

Features defined in the time-domain include measures of the signal's values distribution, such as: their Amplitude, i.e. the difference between the highest and the lowest value; Variance, measuring dispersion around the mean value; Skewness, indicating asymmetry of the distribution; and Kurtosis, showing tail extremity [23]. The VAG signal is symmetric around zero because micro-vibrations from cartilage motion are recorded in both positive and negative directions, canceling each other [19]. As a result, central tendency measures were not calculated. One entropy feature was also calculated, i.e. the log energy entropy [24], being a sum of a logarithm values of the squared signal. It was chosen, because of its parameter-free definition.

In order to calculate characteristics related to the power of the signal, two features were calculated: the root mean square (RMS) value and the rectified average (RAV). Although these features are similar, the RMS tends to be greater, since squared values of the signal are used in its definition.

Ratio of the RMS value to the RAV value is called the Form Factor [25] (sometimes called Shape Factor [26, 27]), and it is one of the *shape* features used in the current research. Other ones, often used in vibration analysis [26, 27], are the crest factor (CF), which is the ratio of maximum absolute value to the RMS value; impulse factor (IF), which is the ratio of maximum absolute value to the RAV value; and Margin Factor (MF, sometimes called Clearance Factor), which is the ratio of absolute maximum value to the absolute generalized mean of the signal.

Additionally, three features describing dynamics of a signal were used. Their definitions include differentiation of a signal. Those features are the mean of absolute differences (MoAD), indicating variability of the signal, and two Hjorth's paramters [28], i.e. Mobility and Complexity. Mobility is a ratio of standard deviation (std) of the differentiated signal to the std of the original signal. It measures "relative average slope" [28] and can be interpreted as representing the mean frequency. Complexity is a ratio of mobility of the differentiated signal to the mobility of the original signal and can represent the change in the frequency: in a pure sine wave, the complexity is equal to one [28].

Another feature defined in the time domain that is related to the frequency is the zero crossings (ZC) feature, i.e. number of times, where consecutive values of the signal are of different sign, normalized by the number of samples in the signal.

Frequency domain features

Informativeness of time- and frequency-domain features can vary significantly for VAG signals [29, 10]. Therefore, additional frequency-domain features were extracted in this study. Four frequency features describing whole spectrum were used [27, 30]: the median frequency (MF), frequency center (FC), root mean square frequency (RMSF) and the root variance frequency (RVF). The MF is the frequency "dividing" the spectrum into two equal parts, i.e. above and below which the spectral power is equal. The FC and the RMSF features indicate changes in the main frequencies, while RVF shows spread of the power across the spectrum.

Additionally, two frequency features widely used in VAG research were calculated: spectral power in the ranges 50–250 Hz (P1) and 250–450 Hz (P2) [13] (used extensively in VAG research, even in different joints [31], and contexts [32], as well as in knee joint diagnosis [33, 34]).

In order to visualize whole spectrum of the VAG signals, frequency range maps (FRM) [19] were generated. Those maps consist of three axes, where *x* and *y*-axes indicate low and high frequency range, while the *z*-axis show informativeness of a feature defined in the *x*-*y* range. Informativeness, however, can be defined in a number of ways [10]. In [19], authors used *z*-axis to visualize the ability of a feature to differentiate groups in a classification problem. In this research, R^2 value of the best model was used. Feature, which informativeness was plotted on the *z*-axis was the relative spectral power. It indicates contribution of specific range to the whole power spectrum, or, in another words, it is a power of specific range divided by total spectral power. Additionally, five more maps were generated, containing the information about the best model selected for specific range: its number and parameters.

MATERIALS AND METHODS

Study participants

A convenience sample of asymptomatic participants was recruited from team sports players, students of the Opole University of Technology, Poland. Only individuals with no history of knee disorder or other diagnosed injury or pathology within the lower extremity were enrolled in the study group. All of the players described their health condition as very good. Finally, 38 male volunteers (aged 22.0 ± 1.1 years, body mass 82.8 ± 10.1 kg, height 186.7 ± 7.9 cm) were included in the study. These values represent the mean ± standard deviation of the participants' demographic characteristics. Before testing, all subjects provided formal consent to participate in the study and to have their results analyzed. The project was approved by the Opole Voivodship Ethics Committee (ethical approval code No. 202/06.06.2013), in accordance with the latest revision and standards of the Helsinki Declaration.

Study protocol

Performed analyses were based on standardized VAG methodology described previously [10]. Briefly, assessment of the patellofemoral joint (PFJ) arthrokinematic motion quality was performed with an accelerometer sensor placed 1 cm above the apex of the patella. This measurement was performed during both unloaded and loaded back squat movements. In total, participants were asked to perform 8 trials: (1) 4 repetitions of bodyweight squats (L0); (2–8) 4 repetitions of 10–70 kg barbell back loaded squats respectively (L10–L70), with one-minute rest between each test. In all these conditions, subjects were instructed to execute the squat from a neutral position (approximately 0° of knee flexion) to the depth of approximately 90° of knee flexion while maintaining heel contact with the floor. The constant velocities of flexion/extension movements were kept at 48 beats per minute with a metronome and the angle of the knee joint was measured using an electrogoniometer. Each squat test lasted 10 seconds, during which four cycles of squats were performed.

Before data collection, each subject performed the squat maneuver within the protocol guidelines. The VAG signals were collected using an acceleration sensor, Brüel and Kjær model 4513B-002 (frequency range 1 Hz to 10 kHz), with a multi-channel Nexus conditioning amplifier (Brüel and Kjær Sound and Vibration Measurement A/S, Denmark). Data were recorded using 12-bit analog-to-digital converter at a sampling frequency of 10 kHz.

Regression models and goodness of fit measures

Four models of increasing complexity have been implemented in this research. Note that the

Table 1. Models used in this research. β_0 and β_1 are the coefficients of the fixed terms: intercept and slope, respectively. Values of S_{0s} and S_{1s} are deviation values from the β_0 and β_1 terms, for specific participants: intercept and slope term, respectively

No.	Name	Equation
1	Simple linear	$X_{sl} = \beta_1 \cdot L_l + e_{sl}$
2	Free term	$X_{sl} = \beta_0 + \beta_1 \cdot L_l + e_{sl}$
3	Random intercept	$X_{sl} = \beta_0 + S_{0s} + \beta_1 \cdot L_l + e_{sl}$
4	Random slope	$X_{sl} = \beta_0 + S_{0s} + (\beta_1 + S_{1s}) \cdot L_l + e_{sl}$

more complex models include the simpler ones. Table 1 summarizes all models.

Conditional R^2 [20] was used in this research as a goodness of fit measure, with modification from [21]:

$$R^2 = \frac{\sigma_f^2 + \sigma_l^2}{\sigma_f^2 + \sigma_l^2 + \sigma_e^2} \qquad (5)$$

where: σ_f^2 is a variance of the fixed effects (can be estimated as variance of values predicted using only fixed terms of the model), $\sigma_l^2 = \left(\sum_j \sum_i \sigma_{lij}^2\right)/n$ [21] is the mean random effects variance, in which i and j stand for the observation and the individual, respectively, and σ_e^2 is a residual variance. Such definition of R^2 measures the variance explained by the model, using both fixed and random effects [20, 21].

Bayesian Information Criterion is defined as follows [18]:

$$BIC = k \ln(n') - 2\ln(\widehat{L}) \qquad (6)$$

where: k is the number of model's parameters, n' is the effective sample size (because of using Restricted Maximum Likelihood, $n' = n - p$, where n is the sample size and p is the number of fixed terms), and $L\hat{}$ is the Restricted Maximum Likelihood value.

Signal's features

Fifteen features defined in the time domain were computed, providing information about the statistical characteristics, power, shape and variability of the signal. Additionally, eight features describing specific characteristics of the spectrum were used. Finally, five frequency range maps [19] were generated, visualizing informativeness of the whole spectrum of the signal. Time-domain based features, along with the detailed definitions, were summarized in the Table 2.

Frequency domain features were calculated on power spectral density (PSD), using periodogram as the estimator [10]. All frequency-domain based features, along with the detailed definitions, were summarized in the Table 3.

RESULTS

Table 4 includes results of the research: models constructed for all features, with corresponding model number, parameters and R^2 measures.

Visualization of an exemplary feature - the log energy entropy - was showed in Figure 2. Here, subplot a) includes visualization of the whole model, with bold black line indicating fixed terms of the model, i.e. the model for new, unknown participant, blue and red area indicating 95% simultaneous and non-simultaneous confidence intervals (CIs), respectively. Simultaneous CIs contain 95% of the whole lines of the responses (features), while non-simultaneous CIs contain 95% of the singular response (feature) observations. Note, that load in this context is normalized by the weight of a participant. Subplots b) and c) show distribution of intercepts and slopes across participants.

Figure 3 show frequency range maps created for the relative spectral power. The Figure includes six subplots: a) showing the informativeness of the feature (Informativeness was defined as the R^2 of the best model describing value of the feature in the varying external load. For each frequency range, four models were constructed and compared using Bayesian Information Criterion, exactly like for the rest of the features), with additional contours roughly indicating areas of similar informativeness. The same contour maps were also plotted on the rest of the subplots. The b) subplot shows number of the best model number, c) and d) show intercept mean and std values, respectively. Subplots e) and f) show, respectively, slope mean and std values. Note, that if the best

Table 2. Summary of the time-domain features

No.	Feature	Definition
1	Amplitude	$max(x) - min(x)^{\dagger}$
2	Variance	$\frac{\sum_{i=1}^{N}(x_i - \mu)^2}{(N-1)\cdot\sigma^2}$ ‡
3	Skewness	$\frac{\sum_{i=1}^{N}(x_i - \mu)^3}{(N-1)\cdot\sigma^3}$
4	Kurtosis	$\frac{\sum_{i=1}^{N}(x_i - \mu)^4}{(N-1)\cdot\sigma^4}$
5	Log energy entropy	$\sum_{i=1}^{N} ln|x_i|^2$
6	Root mean square	$\sqrt{\frac{1}{N}\sum_{i=1}^{N}x_i^2}$
7	Rectified average	$\frac{1}{N}\sum_{i=1}^{N}|x_i|$
8	Form factor	$\frac{\sqrt{\frac{1}{N}\sum_{i=1}^{N}x_i^2}}{\frac{1}{N}\sum_{i=1}^{N}|x_i|}$
9	Crest factor	$\frac{max|x_i|}{\sqrt{\frac{1}{N}\sum_{i=1}^{N}x_i^2}}$
10	Impulse factor	$\frac{max|x_i|}{\frac{1}{N}\sum_{i=1}^{N}|x_i|}$
11	Margin factor	$\frac{max|x_i|}{\left(\frac{1}{N}\sum_{i=1}^{N}\sqrt{|x_i|}\right)^2}$
12	Mean of absolute differences	$\frac{1}{N}\sum_{i=1}^{N-1}|x_i'|$ §
13	Mobility	$\frac{\sigma_{x'}}{\sigma_x}$
14	Complexity	$\frac{\sigma_{x''}}{\sigma_{x'}}/\frac{\sigma_{x'}}{\sigma_x}$
15	Zero crossings	$\frac{1}{N}\sum_{i=1}^{N-1}\mathbb{I}(x_i \cdot x_{i+1} < 0)$

Note: † x is the signal ‡ N, μ, and σ indicate the sample count, mean, and standard deviation of the signal x, respectively. § $x_i' = x_{i+1} - x_i$ §

DISCUSSION

Interpretation of constructed models

Time domain features

Range of the vibroarthrogram, i.e. the Amplitude feature, did not prove to be much informative in the external load context. With the R^2 score model for specific range did not assume some parameters, their values were not plotted (see, for example, range 3500–4000 Hz in Figure 3f)).

of less than 0.4, it actually proved to be one of the least informative features. Low informativeness of the amplitude could be explained by the possible existence of outliers, for which the amplitude feature is extremely vulnerable.

The Variance feature, indicating dispersion of the values and power of the signal, achieved the R^2 value of more than 0.9, proving to be one of the most informative features. Mean slope of the model, so the β_1 parameter, indicated positive correlation with the external load in most participants. The positive β_1 for Variance suggests increased signal energy dissipation under load,

Table 3. Summary of the frequency-domain features

No.	Feature	Definition	Remarks
16	Median frequency	Frequency that divides the spectrum into two equal parts; i.e. above and below which, spectral power is equal.	
17	Frequency center	$$\dfrac{\sum f \cdot P(f)}{\sum P(f)}$$	Both sums are over the whole spectrum. $P(f)$ is spectral power of the specific, $f - th$ frequency component.
18	Root mean square frequency	$$\sqrt{\dfrac{\sum f^2 \cdot P(f)}{\sum P(f)}}$$	
19	Root variance frequency	$$\sqrt{\dfrac{\sum (f - FC)^2 \cdot P(f)}{\sum P(f)}}$$	FC is the frequency center.
20	P1	$$\sum_{f=50\,Hz}^{250\,Hz} P(f)$$	
21	P2	$$\sum_{f=250\,Hz}^{450\,Hz} P(f)$$	
22	Relative spectral power†	$$\sum_{f_L}^{f_U} P(f) \,/\, \sum_{f\,min}^{f_{max}} P(f)$$	f_{min} and f_{max} are the minimum and the maximum frequency values of the power spectrum, respectively.

Note: † Feature used to generate the frequency range map.

likely reflecting heightened mechanical stress in the joint. Note, however, that the S_1 value turn out to be greater than the β_1. It means that for some participants, Variance of the VAG signal is negatively correlated with the load.

Asymmetry of the distribution, measured by the Skewness feature, turn out to be not informative at all, with the R^2 lower than 0.2. It shows that symmetry of the signal does not change with varying external load.

Kurtosis feature, indicating tail extremity, obtained R^2 of 0.64. It is not high, especially compared to other features. However, to model the feature, the third model was used, i.e. model without random slope parameter. Negative value of the β_1 shows that for most signals, Kurtosis is negatively correlated with external load, i.e. with the increasing load, the Kurtosis decreases (distribution's tails become smaller).

Log Energy Entropy turn out to be positively correlated with the external load, with positive value of the β_1 parameter. It aligns with increased signal unpredictability due to frictional changes during higher loading. Note, that the LEE was calculated for a raw signal, with a plethora of values lower than one. Therefore, for this kind of signals, values of the LEE feature tend to be negative. It is clearly indicated by the β_0 and S_0 parameters of the model, proving consistent negative intercept. Note, however, that the S_1 parameter is greater

than the β_1, indicating that for some participants, the LEE feature is correlated with external load negatively. Note also, that the informativeness of the LEE feature turn out to be one of the highest, with R^2 of more than 0.9.

Two power features, so the Root Mean Square and the Rectified Average proved to be highly informative (with $R^2 > 0.9$ for both) and positively correlated with the external load, with positive β_1. They indicate greater overall signal magnitude, consistent with higher contact forces and frictional energy under external load, confirming conclusions derived from the Variance feature. Note, however, that for both features S_1 is greater than β_1, proving that for some vibroarthrograms RMS and ARV are negatively correlated with the load.

Form Factor, as the only one of all the shape features, proved to be positively correlated with the load. However, with $R^2 < 0.7$, it cannot be considered highly informative. This outcome is consistent with prior research by Andersen et al. [17].

Even lower R^2 value was achieved by the Crest Factor. However, for both features, the third model (without the random slope parameter), was chosen. This could indicate consistency of the slope between study participants. The Impulse Factor proved to be negatively correlated with the load for most participants, and its R^2 value of about 0.85 indicate relatively high informativeness. The last feature describing the shape of

Table 4. Results table for the scalar features. Note, that frequency range maps were not included in the table

Feature	R^2	Model number	β_0	S_0	β_1	S_1	e
Amplitude	0.38	3	7.3e+0	7.1e-1	5.1e-1	-	9.2e-1
Variance	0.91	4	2.1e-2	1.8e-2	1.4e-2	2.8e-2	1.2e-2
Skewness	0.16	3	-4.2e-1	6.5e-1	5.0e-1	-	1.5e+0
Kurtosis	0.64	3	2.9e+2	2.0e+2	-6.1e+1	-	1.5e+2
Log energy entropy	0.93	4	-7.3e+0	5.3e-1	2.5e-1	4.0e-1	2.0e-1
Root mean square	0.91	4	1.3e-1	5.5e-2	3.9e-2	6.5e-2	3.0e-2
Rectified average	0.92	4	5.3e-2	2.2e-2	1.3e-2	2.1e-2	9.4e-3
Form factor	0.68	3	2.6e+0	4.9e-1	9.4e-2	-	3.4e-1
Crest factor	0.62	3	3.0e+1	8.2e+0	-4.7e+0	-	6.5e+0
Impulse factor	0.85	4	8.1e+1	2.9e+1	-1.2e+1	1.8e+1	1.5e+1
Margin factor	0.85	4	1.2e+2	4.4e+1	-1.4e+1	2.4e+1	2.2e+1
Mean of absolute differences	0.94	4	3.8e-2	1.9e-2	7.5e-3	1.8e-2	7.3e-3
Mobility	0.80	4	7.9e-1	9.5e-2	-4.6e-2	8.8e-2	6.9e-2
Complexity	0.72	4	1.8e+0	1.3e-1	1.1e-1	1.9e-1	1.6e-1
Zero crossings	0.84	4	2.3e-1	2.2e-2	-2.8e-3	2.2e-2	1.5e-2
Median frequency	0.73	4	7.8e+2	1.3e+2	-9.1e+1	1.5e+2	1.3e+2
Frequency center	0.81	4	1.1e+3	1.7e+2	-9.0e+1	1.7e+2	1.2e+2
Root mean square frequency	0.80	4	1.5e+3	2.0e+2	-8.5e+1	1.7e+2	1.4e+2
Root variance frequency	0.67	3	9.6e+2	1.2e+2	-2.7e+1	-	8.8e+1
P1	0.84	4	2.0e-2	1.8e-2	1.9e-2	2.0e-2	1.3e-2
P2	0.87	4	2.7e-2	2.3e-2	2.4e-2	3.5e-2	1.8e-2
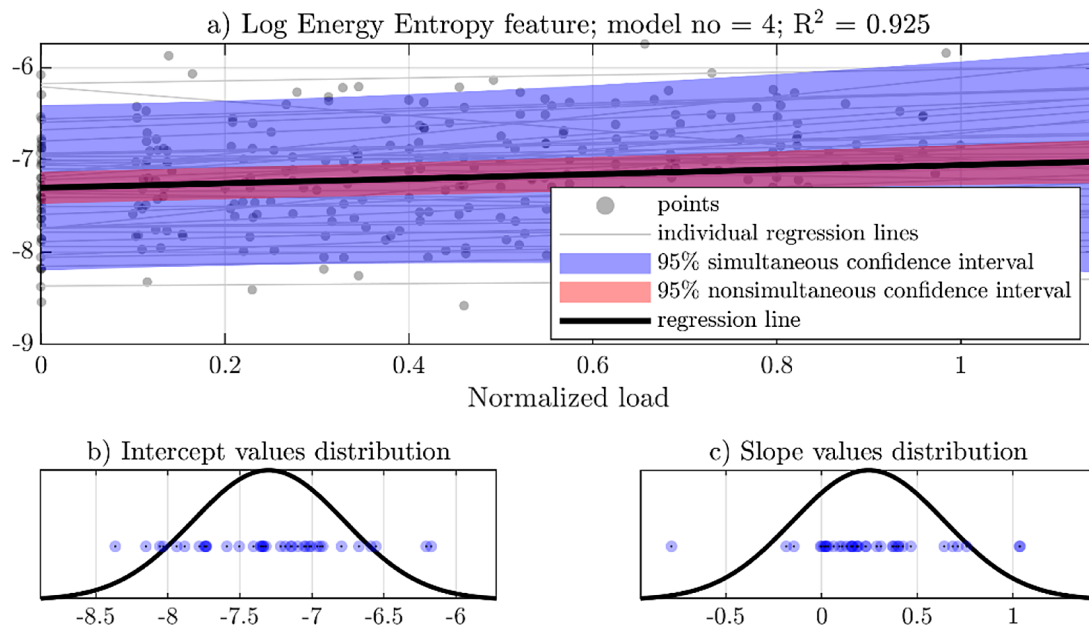
Figure 2. Visualization of the log energy entropy feature's model

the vibroarthrogram, so the Margin Factor, also achieved R^2 value of about 0.85. Also, similarly to the Impulse Factor, it turned out to be negatively correlated with the external load, however, not really consistently across the participants – note

higher absolute value of the S_1 parameters than the β_1 for both features. Note, that the Crest, the Impulse and the Margin factors have very similar definitions, differing only in the type of the average in the denominator (see Table 2). Negative
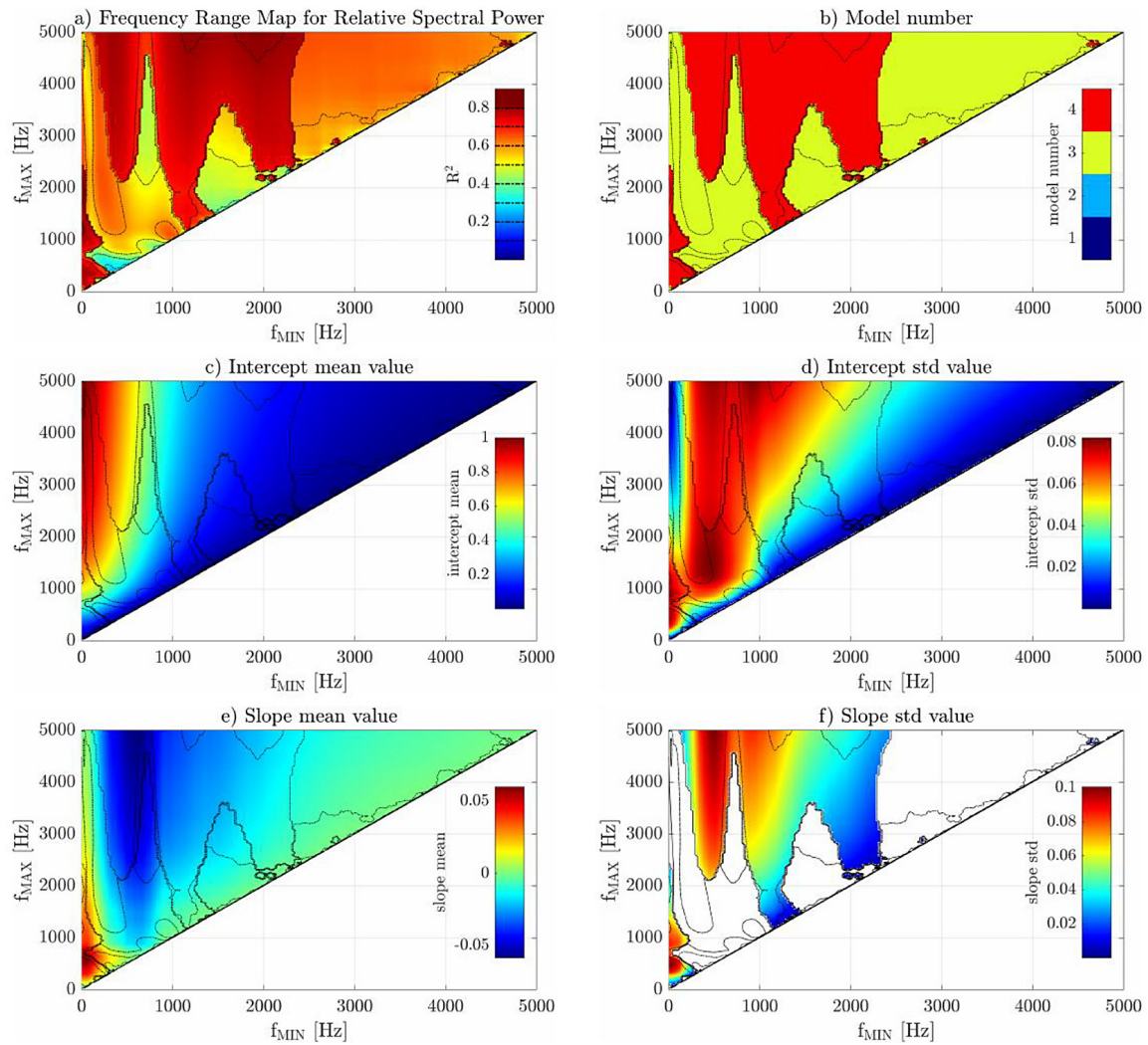
Figure 3. Frequency range maps for the relative spectral power feature

correlations with the load can be then explained through the models developed for the RMS and the RAV features: both proved to be positively correlated with the load.

Variability of the VAG, measured using the MoAD feature, proved to be extremely informative, with the R^2 of about 0.94, and positively correlated with the load. That further confirms that power of the signal increases with the external load.

Hjorth's parameters turn out to be moderately informative, with the R^2 of 0.80 and 0.72 for the Mobility and the Complexity feature, respectively. Mobility feature proved to be negatively correlated with the load, indicating that with the increase of the load, spectrum of the signal tends to lower values. Complexity, on the other hand, turn out to be positively correlated, meaning that with greater load, spectrum changes more.

The last time-domain feature, also referring to the instantaneous frequency, is the Zero Crossings

feature. With a R^2 value of about 0.84 it can be considered moderately informative. With negative β_1 value, this feature confirms conclusions of the Hjorth's mobility feature - frequency components of the vibroarthrogram tend to decrease with the increase of the external load, reflecting potentially lowered joint mobility under heavier loads. Note, however, that the value of the S_1 parameter is much greater, indicating that the slope is not consistent across participants.

Frequency domain features and frequency range maps

Features defined in the frequency domain, which describe the whole spectrum, so the Median Frequency ($R^2 = 0.73$), Frequency Center ($R^2 = 0.81$) and the Root Mean Square Frequency ($R^2 = 0.81$) further confirm that with the increase of the load, power of the signal tends to concentrate

in lower frequencies. For all those features, β_1 parameter was negative. This seem to be consistent with previous findings by Andersen et al. [17], in which Mean Power Frequency decreased statistically significantly with external load. Note, however, that the S_1 was greater than the absolute value of the β_1, indicating that there were some participants with positive correlations. As an additional confirmation, on Figure 4, the mean values of periodograms were plotted, in the function of the external load. A tendency of the lower frequencies (below the 1 kHZ) to grow in power is clearly visible. Also, the Root Mean Variance Frequency feature is negatively correlated to the load, which means that with the heavier weight, the power tends to be less spread across the spectrum, or in another words, more concentrated around the Frequency Center. Since the third model was used with the RMVF feature, it can be assumed, that the negative correlation is consistent across the participants.

Both P1 and P2 features, representing power in 50–250 Hz and 250–450 Hz, respectively, seem to be positively correlated with external load. Also, both features are quite informative, with R^2 above 0.8. This result is consistent with previous work by Ołowiana et al. [15].

Maps generated for the Relative Spectral Power feature (Figure 3) show a diversity of informativeness across the spectrum. Subplot *a* shows R^2 values of the constructed models, while subplot *b* presents model number. As one could expect, the most informative models were the most complex ones - compare dark red areas on subplot *a* with subplot *b*. Subplots *c* and *d* show

intercept mean and standard deviation values across participants, respectively. Lower and narrow frequency ranges have generally lower intercept values. Since Relative Spectral Power is normalized to the whole spectrum, narrow ranges result in relatively low values. However, those patterns are not as clearly visible in the subplot *d*. In the lower frequencies of the spectrum (lower left corner of the map), there is a clear increase in standard deviation values. It could be explained by different model used in those frequency ranges – see subplot *a*. Subplots *e* and *f* confirm earlier observations, that lower frequency ranges (below 1000 Hz) tend to be positively correlated with the external load, contributing more to the power of the VAG's spectrum. In contrast, higher frequency ranges show lower or even negative slope values, indicating that their contribution to the power spectrum decreases with greater external load.

Clinical significance

Synovial joints are optimized to function under physiological loading conditions. They then provide an extremely low coefficient of kinetic friction, which translates into low vibration levels observed in recorded VAG signals. From tribological point of view the ability of the articular surfaces to move smoothly against each other with low frictional noise indicates optimal arthrokinematic motion and as a result contributes to slow wear of articular cartilage [35].

As expected, the presented results indicate that with an increase in the applied external load there is a progressive rise in the power of the
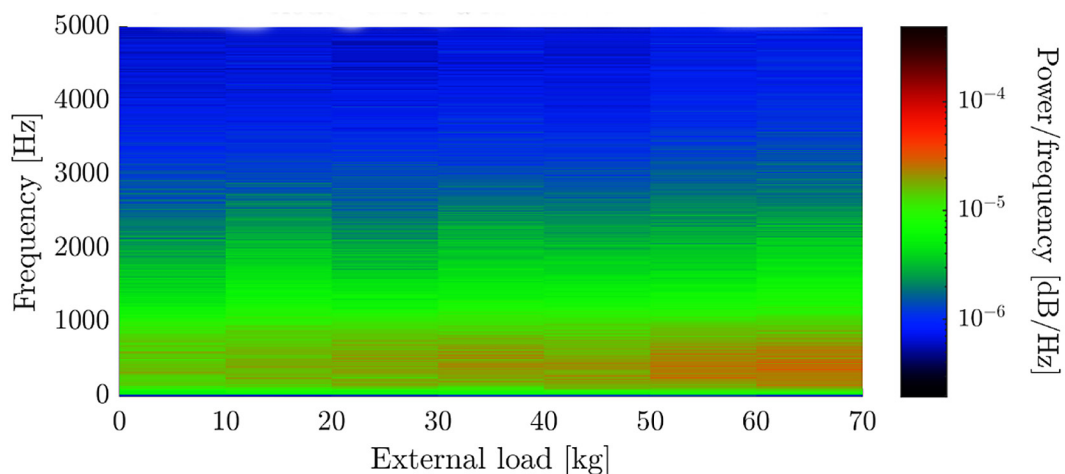
Figure 4. Mean values of the periodogram as the function of the external load. Note, that for increasing load, power (red area) in the low frequencies also increases.

signal, most likely related to a growth of contact stress and kinetic friction. This confirms conclusions from previous works by Ołowiana et al. [15] and Andersen et al. [17]. Nevertheless, this increase is lower than expected, especially since Lizhang et al. [36] showed that a squat performed under a 35% of body weight external load yielded a more than 40% increase in PFJ stress across all knee flexion angles. Thus, our results seem to show that healthy synovial joints have efficient mechanisms to adapt to the load acting on them, most likely, by altering the lubrication mechanism [37]. This is in line with research by Gharehbaghi et al. [16], which showed no significant differences in healthy subjects' knee health scores between loaded and unloaded knee joint movements. Direct comparison between this score and specific features extracted in the current study is difficult, since the score is a composite of multiple features. Still, one could argue, that the character of changes in VAG signals differ between progressing knee joint degeneration and increasing external load.

Nonetheless, the conducted analyses confirmed that VAG method possess not only high accuracy and specificity when differentiating synovial joints' deteriorations, but also is sensitive for identifying the changes in arthrokinematics related to the level of the joint load [38]. Since knee joint vibroarthrography is known to be a repeatable examination [39], conducted study implies that VAG signals constitute a helpful tool for clinicians for evaluating joint function of specific person, for example, over time.

Further research directions

While this study focused on normalized load, future research could examine the impact of participant's absolute body mass and height on VAG signal responses, as these factors could potentially influence joint mechanics and frictional dynamics. Additionally, investigations into other demographics (e.g., gender, age groups, physical activity) would enhance generalizability. Testing VAG in different movement types, such as lunges or step-ups, could help validate the methodology beyond squats. Furthermore, longitudinal studies tracking VAG signals of specific participants over time would provide insights into the progression of joint degeneration, offering potential for early detection and monitoring of biomechanical changes in clinical settings.

CONCLUSIONS

In this research, selected features of the vibroarthrogram were modeled in the context of external load. Results of this study can be used in the future research considering joint friction measured by the vibroarthrogram. The most important conclusions that can be drawn from the research include correlations between specific features of the VAG signal and the external load:

- positive correlation for the power of the signal, measured by the time-domain Variance ($\beta_1 = 1.4e{-}2$; $R^2 = 0.91$), RMS ($\beta_1 = 3.9e{-}2$; $R^2 = 0.91$), RAV ($\beta_1 = 1.3e{-}2$; $R^2 = 0.92$) and MoAD ($\beta_1 = 7.5e{-}3$; $R^2 = 0.94$) features and the frequency-domain P1 ($\beta_1 = 1.9e{-}2$; $R^2 = 0.84$) and P2 ($\beta_1 = 2.4e{-}2$; $R^2 = 0.87$) features. Also, Absolute Power of the spectrum proved to be positively correlated for practically all frequency ranges.
- negative correlation between three shape features: the Crest Factor ($\beta_1 = -4.7e0$; $R^2 = 0.62$), the Impulse Factor ($\beta_1 = -1.2e{+}1$; $R^2 = 0.85$) and the Margin Factor ($\beta_1 = -1.4e{+}1$; $R^2 = 0.85$).
- negative correlation between central tendencies of the spectrum, measured by the Median Frequency ($\beta_1 = -9.1e{+}1$; $R^2 = 0.73$), Frequency Center ($\beta_1 = -9.0e{+}1$; $R^2 = 0.73$) and the RMS Frequency ($\beta_1 = -8.5e{+}1$; $R^2 = 0.80$) features. It can also be seen on Frequency Range Maps measured for the Relative Spectral Power.

REFERENCES

1. Micheo W., Rodríguez-Santiago B., Sepulveda-Irizarry F., Castillo B. Knee Injuries. In: Essential Sports Medicine. 2021. https://doi.org/10.1007/978-3-030-64316-4_16

2. Logerstedt D.S., Ebert J.R., MacLeod T.D., Heiderscheit B.C., Gabbett T.J., Eckenrode B.J. Effects of and Response to Mechanical Loading on the Knee. Sports Medicine. 2022; 52(2): 201–235. https://doi.org/10.1007/s40279-021-01579-7

3. Liu J. Prevention and Rehabilitation of Knee Joint Injury. Investigación Clínica. 2020; 61(2): 645–655.

4. Levangie P.K., Norkin C.C. Joint Structure and Function: A Comprehensive Analysis. F.A. Davis Co; 2005.

5. Armiento A.R., Alini M., Stoddart M.J. Articular fibrocartilage - why does hyaline cartilage fail to repair? Advanced Drug Delivery Reviews. 2019; 146: 289–305. https://doi.org/10.1016/j.addr.2018.12.015

6. Liew I., Khan W.S. Cartilage Injuries in the Knee. In: Orthopedics of the Upper and Lower Limb. 2020. https://doi.org/10.1007/978-3-030-43286-7_21

7. Widmalm S., Westesson P., Brooks S.L., Hatala M.P., Paesani D. Temporomandibular joint sounds: correlation to joint structure in fresh autopsy specimens. American Journal of Orthodontics and Dentofacial Orthopedics. 1992; 101(1): 60–69. https://doi.org/10.1016/0889-5406(92)70083-M

8. Karpiński R., Krakowski P., Jonak J., Machrowska A., Maciejewski M., Nogalski A. Diagnostics of articular cartilage damage based on generated acoustic signals using ANN—Part I: Femoral-tibial joint. Sensors. 2022; 22(6): 2176. https://doi.org/10.3390/s22062176

9. Karpiński R., Krakowski P., Jonak J., Machrowska A., Maciejewski M., Nogalski A. Diagnostics of articular cartilage damage based on generated acoustic signals using ANN—Part II: patellofemoral joint. Sensors. 2022; 22(10): 3765. https://doi.org/10.3390/s22103765

10. Łysiak A. Automatic Diagnosis of the Patient's Knee Joint Using Selected Methods of Vibroarthrographic Signal Analysis [PhD thesis]. Opole: Opole University of Technology, 2023. https://doi.org/10.13140/RG.2.2.34386.77765

11. Befrui N., Elsner J., Flesser A., Huvanandana J., Jarrousse O., Le T.N., Müller M., Schulze W.H.W., Taing S., Weidert S. Vibroarthrography for early detection of knee osteoarthritis using normalized frequency features. Medical & Biological Engineering & Computing. 2018; 56(8): 1499–1514. https://doi.org/10.1007/s11517-018-1785-4

12. Machrowska A., Karpiński R., Maciejewski M., Jonak J., Krakowski P. Application of EEMD-DFA algorithms and ANN classification for detection of knee osteoarthritis using vibroarthrography. Applied Computer Science. 2024; 20(2): 90–108. https://doi.org/10.35784/acs-2024-18

13. Kręcisz K., Bączkowicz D. Analysis and multiclass classification of pathological knee joints using vibroarthrographic signals. Computer Methods and Programs in Biomedicine. 2017; 154: 37–44. https://doi.org/10.1016/j.cmpb.2017.10.027

14. Falkowski K., Madej W., Hubeny J. Single intraarticular injection of high-molecular and highly concentrated hyaluronic acid improves arthrokinematics in the knee joint, resulting in a significant clinical outcome. Osteoarthritis and Cartilage. 2024; 32: S590-S591. https://doi.org/10.1016/j.joca.2024.02.872

15. Ołowiana E., Selkow N., Laudner K., Puciato D., Bączkowicz D. Vibroarthrographic analysis of patellofemoral joint arthrokinematics during squats with increasing external loads. BMC Sports Science, Medicine and Rehabilitation. 2020; 12(1): 51. https://doi.org/10.1186/s13102-020-00201-z

16. Gharehbaghi S., Whittingslow D.C., Ponder L.A., Prahalad S., Inan O.T. acoustic emissions from loaded and unloaded knees to assess joint health in patients with juvenile idiopathic arthritis. IEEE Journal of Biomedical and Health Informatics. 2021; 25(9): 3618–3626. https://doi.org/10.1109/JBHI.2021.3081429

17. Andersen R.E., Arendt-Nielsen L., Madeleine P. Knee Joint Vibroarthrography of asymptomatic subjects during loaded flexion-extension movements. Medical & Biological Engineering & Computing. 2018; 56(12): 2301–2312. https://doi.org/10.1007/s11517-018-1856-6

18. Wit E., van den Heuvel E., Romeijn J. 'All Models Are Wrong...': an introduction to model uncertainty. Statistica Neerlandica. 2012; 66(3): 217–236. https://doi.org/10.1111/j.1467-9574.2012.00530.x

19. Łysiak A., Froń A., Bączkowicz D., Szmajda M. Vibroarthrographic signal spectral features in 5-class knee joint classification. Sensors. 2020; 20(17): 5015. https://doi.org/10.3390/s20175015

20. Nakagawa S., Schielzeth H. A general and simple method for obtaining r2 from generalized linear mixed-effects models. Methods in Ecology and Evolution. 2013; 4(2): 133–142. https://doi.org/10.1111/j.2041-210x.2012.00261.x

21. Johnson P.C. Extension of Nakagawa & Schielzeth's R2GLMM to random slopes models. Methods in Ecology and Evolution. 2014; 5(9): 944–946. https://doi.org/10.1111/2041-210X.12225

22. Gohain P.B., Jansson M. Scale-invariant and consistent Bayesian information criterion for order selection in linear regression models. Signal Processing. 2022; 196: 108499. https://doi.org/10.1016/j.sigpro.2022.108499

23. Westfall P.H. Kurtosis as Peakedness, 1905–2014. R.I.P. The American Statistician. 2014; 68(3): 191–195. https://doi.org/10.1080/00031305.2014.917055

24. Sharma M., Sharma P., Bilas R., Gadre V.M. Double density dual-tree complex wavelet transform-based features for automated screening of knee-joint vibroarthrographic signals. In: Machine Intelligence and Signal Analysis. 2019. https://doi.org/10.1007/978-981-13-0923-6_24

25. Aarts R.M. Tracking and estimation of frequency, amplitude, and form factor of a harmonic time series

[Lecture Notes]. IEEE Signal Processing Magazine. 2021; 38(5): 86–91. https://doi.org/10.1109/MSP.2021.3090681

26. Yiakopoulos C.T., Gryllias K.C., Antoniadis I.A. Rolling element bearing fault detection in industrial environments based on a k-means clustering approach. Expert Systems with Applications. 2011; 38(3): 2888–2911. https://doi.org/10.1016/j.eswa.2010.08.083

27. Caesarendra W., Tjahjowidodo T. A review of feature extraction methods in vibration-based condition monitoring and its application for degradation trend estimation of low-speed slew bearing. Machines. 2017; 5(4): 21. https://doi.org/10.3390/machines5040021

28. Hjorth B. EEG Analysis based on time domain properties. Electroencephalography and Clinical Neurophysiology. 1970; 29(3): 306–310. https://doi.org/10.1016/0013-4694(70)90143-4.

29. 2Kręcisz K. Bączkowicz D., Łysiak A., Szmajda M., Kawala-Sterniuk A. Correlation between linear and non-linear vibroartrographic parameters. Przegląd Elektrotechniczny. 2023; 1(7): 182–187. https://doi.org/10.15199/48.2023.07.33

30. Han T., Yang B., Choi W., Kim J. Fault diagnosis system of induction motors based on neural network and genetic algorithm using stator current signals. International Journal of Rotating Machinery. 2006; 2006: 1–13. https://doi.org/10.1155/IJRM/2006/61690

31. Bączkowicz D., Kręcisz K. Vibroarthrography in the evaluation of musculoskeletal system - a pilot study. Ortopedia Traumatologia Rehabilitacja. 2013; 15(5): 407–416. https://doi.org/10.5604/15093492.1084242

32. Bączkowicz D., Majorczyk E., Kręcisz K. Age-related impairment of quality of joint motion in vibroarthrographic signal analysis. BioMed Research International. 2015; 2015: 1–7. https://doi.org/10.1155/2015/591707

33. Bączkowicz D., Majorczyk E. Joint motion quality in vibroacoustic signal analysis for patients with patellofemoral joint disorders. BMC Musculoskeletal Disorders. 2014; 15(1): 426. https://doi.org/10.1186/1471-2474-15-426

34. Łysiak A., Froń A., Bączkowicz D., Szmajda M. The new descriptor in processing of vibroacoustic signal of knee joint. IFAC-PapersOnLine. 2019; 52(27): 335–340. https://doi.org/10.1016/j.ifacol.2019.12.683

35. Bączkowicz D., Kręcisz K., Borysiuk Z. Analysis of patellofemoral arthrokinematic motion quality in open and closed kinetic chains using vibroarthrography. BMC Musculoskeletal Disorders. 2019; 20(1): 48. https://doi.org/10.1186/s12891-019-2429-z

36. 3Lizhang J., Fisher J., Jin Z., Burton A., Williams S. The effect of contact stress on cartilage friction, deformation and wear. proceedings of the institution of mechanical engineers, Part H: Journal of Engineering in Medicine. 2011; 225(5): 461–475. https://doi.org/10.1177/2041303310392626

37. Singh N. Synovial joints and lubrication mechanisms. International Journal of Computational and Applied Mathematics. 2017; 12(1): 29–33

38. Sher N.M., Nazli R., Zafar H., Fatima S. Effects of lipid based multiple micronutrients supplement on the birth outcome of underweight pre-eclamptic women: a randomized clinical trial. Pakistan Journal of Medical Sciences. 2021; 38(1). https://doi.org/10.12669/pjms.38.1.4396

39. Kalo K., Niederer D., Sus R., Sohrabi K., Groß V., Vogt L. Reliability of vibroarthrography to assess knee joint sounds in motion. Sensors. 2020; 20(7): 1998. https://doi.org/10.3390/s20071998